

## Grain Refinement of Cu-Zn-Al Shape Memory Alloys

J. S. LEE\* AND C. M. WAYMAN

*Department of Metallurgy and Mining Engineering, University of Illinois at Urbana-Champaign, 1304 W. Green Street, Urbana, Illinois 61801*

Various dopants, such as boron and its compounds and pure elements such as Zr, Ti, V and Cr, were added to two commercial, copper-based shape memory alloys (70.7% Cu-25.7% Zn-3.58% Al [alloy X] and 65.6% Cu-31.4% Zn-2.95% Al-0.1% Zr [alloy Y]) in order to identify their grain refining abilities. Different annealing schedules were given to certain of the grain-refined alloys to observe their grain growth rate. Boron and various borides provided some degree of grain refinement, although not extensive. Zr and Ti produced the most grain refinement. Moreover, Zr suppressed the grain growth rate to virtually zero even after 6 h annealing at 800°C. The Ti-doped alloys had a relatively larger grain growth rate. Zr-rich second-phase particles, observed at the grain boundaries of Zr-doped alloys, are believed to be responsible for grain refinement. The formability of all alloys investigated was studied by hot-rolling with intermediate annealing. A 98% reduction, leading to a final thickness of 0.254 mm could be achieved for all the alloys. For the 0.91% Zr-doped alloys, a 98% reduction did not increase the grain growth rate. Zr-, Ti-, V-, and Cr-doped alloys were tensile-fractured as well as impact-fractured *in situ* in an Auger vacuum system. These alloys all showed a ductile transgranular fracture mode; no grain boundary segregation was detected. An equation to predict the  $M_s$  temperature in Cu-Zn-Al alloys was obtained by analyzing previous data using a first-order linear regression computer program.

### Introduction

Shape memory alloys (SMA) have been studied extensively in recent years and much knowledge has been gained of them and their martensitic transformation characteristics, which are closely related to the shape memory effect (SME). Among the various SMA, NiTi and copper-based alloys are the most popular systems and both have been used extensively in different applications. NiTi alloys usually have good mechanical properties, due to their small grain size and low elastic anisotropy ( $A = 2C_{44}/$

\* Current address is GTE Corp., Towanda, PA 18848.

$[C_{11}-C_{12}] \approx 2$  [1]. However, because of high materials costs and difficulties involved in alloy preparation and fabrication, their use in many applications has been limited. On the other hand, the copper-based alloys have relatively inexpensive materials costs and easier formability. Thus, much attention has been turned to the copper-based SMA. However, a major problem with the copper-based SMA is their large intrinsic grain size and high elastic anisotropy ( $A = 13$  in some cases), which leads to ductility problems and a decrease in shape memory recovery [2].

In the past, several different approaches have been used to control grain size in copper-based SMA. One method has been to carefully control the temperature and time of solution treatment in order to cause the retention of a small amount of the  $\alpha$  phase just prior to quenching, with the presence of the second phase intended to inhibit grain growth of the parent  $\beta$  phase. Another approach, that used in the current study, is the addition of a fourth element in an effort to provide more  $\beta$ -phase nucleation sites [3]. Recently, efforts to refine the grain size by adding quaternary elements have been attempted for Cu-Zn-Al [4-6] and Cu-Al-Ni [1, 7] alloys.

The objectives of the present work were fourfold: 1) to identify the best grain refiners for copper-based SMA; 2) to observe the grain growth rates in various fine-grained copper-based SMA; 3) to study the formability and other mechanical properties of various fine-grained SMA; and 4) to study why grain refinement leads to superior mechanical behavior.

## Experimental

Various fine-grained copper-based SMA have been developed. Certain dopants in small quantities were added to two commercial copper-based SMA containing 70.7% Cu-25.7% Zn-3.58% Al and 65.6% Cu-31.4% Zn-2.95% Al-0.01% Zr (wt. %). These alloys were obtained in rod form from Memory Metals, Inc., Stamford, CT. The first (Zr-free) copper-based SMA (alloy X) typically featured a large grain size of about 1 mm, with a martensitic transformation temperature ( $M_s$ ) at 107°C. The second alloy (alloy Y) contained 0.1% Zr and typically featured a smaller grain size, in the range from 150 to 300  $\mu\text{m}$ , with the  $M_s$  below -192°C. Various empirically chosen additives such as B, AlB<sub>2</sub>, TiB<sub>2</sub>, CrB<sub>2</sub>, NiB, Zr, Ti, V, and Cr were added to alloy X in order to identify the best candidates to refine the grain size; only Zr, Ti, V, and Cr were added to alloy Y. The quantities of dopants varied from 1% to 0.01% (wt.%). However, the addition of a minute amount of dopant should not be considered trivial. Moreover, mixing problems arise because of the high melting point of some of the boron compounds. As a precaution, master alloys containing

boron and boron compounds were prepared by "raw" melting of the dopants with the base alloys followed by remelting in an induction unit. For the dopants Zr, Ti, V, and Cr, which were mixed in larger quantities, a one-step melting process in the induction unit gave good mixing results.

The melted alloys were sealed in argon-filled quartz tubes and homogenized at 800°C for 12 h followed by a room-temperature water quench. The ingots were then rolled, in air, to plates of 1.27 mm thickness. Intermediate annealing at 600°C was required every two to three passes. Specimens with dimensions of 25.4 mm × 1.27 mm × 1.27 mm were cut from the final plate form. After solution treatment at 800°C for various times, followed by a step quench to 150°C (and holding for 10 min) before cooling to room temperature, electrical resistivity measurements were performed to determine transformation temperatures. Grain sizes were determined through optical microscopy for each specimen after mechanical polishing, although no particular care was exercised here in that grain size measurements were only of primary concern.

Some of the fine-grained alloys were fractured in air and studied fractographically by SEM. The same alloys were also fractured *in situ* in an Auger electron vacuum chamber and their fracture surfaces immediately studied to determine whether there was any compositional segregation. Preliminary TEM studies were conducted on one of the finest grained alloys.

## Results and Discussion

Table 1 lists the nominal chemical compositions of all alloys studied, their  $M_s$  temperatures, and average grain sizes. All alloys listed were annealed at 800°C for 5 min, followed by a step quench to oil at 150°C, and then cooled to room temperature. The grain refinement effect of each dopant will be discussed separately.

### B ADDITIONS

Three different B-doped alloys were melted from a master alloy of composition of 70.7% Cu-25.7% Zn-3.58% Al-0.55% B (XB alloy). These alloys contained B in amounts 0.051% (XB-1), 0.031% (XB-2), and 0.011% (XB-3). The B-free base alloy had a grain size of about 1 mm after 5 min solution treatment at 800°C (Fig. 1). Under the same annealing conditions, XB-1 had a grain size of 250  $\mu\text{m}$ ; XB-2, 350  $\mu\text{m}$ ; and XB-3, 500  $\mu\text{m}$ . The master alloy had a smaller grain size, 120  $\mu\text{m}$ . Martensite was observed in all the B-doped alloys, as shown in Fig. 2, but no distinct second phase

TABLE I  
Nominal Chemical Compositions,  $M_s$  Temperatures, and Average Grain Size of Alloys Studied<sup>a</sup>

Alloy	Composition (parts by weight)	$M_s$ (°C)	Grain size (μm)
X	70.7 Cu-25.7 Zn-3.58 Al	107	920
XB-1	70.7 Cu-25.7 Zn-3.58 Al + 0.051 B	120	250
XB-2	70.7 Cu-25.7 Zn-3.58 Al + 0.031 B	—	350
XB-3	70.7 Cu-25.7 Zn-3.58 Al + 0.011 B	133	500
XA1B <sub>2</sub> -1	70.7 Cu-27.7 Zn-3.58 Al + 0.051 AlB <sub>2</sub>	130	300
XA1B <sub>2</sub> -2	70.7 Cu-27.7 Zn-3.58 Al + 0.03 AlB <sub>2</sub>	127	640
XA1B <sub>2</sub> -3	70.7 Cu-27.7 Zn-3.58 Al + 0.01 AlB <sub>2</sub>	132	730
XTiB <sub>2</sub> -1	70.7 Cu-25.7 Zn-3.58 Al + 0.051 TiB <sub>2</sub>	142	760
XTiB <sub>2</sub> -2	70.7 Cu-25.7 Zn-3.58 Al + 0.03 TiB <sub>2</sub>	136	780
XTiB <sub>2</sub> -3	70.7 Cu-25.7 Zn-3.58 Al + 0.01 TiB <sub>2</sub>	127	900
XCrB <sub>2</sub> -1	70.7 Cu-25.7 Zn-3.58 Al + 0.052 CrB <sub>2</sub>	135	550
XCrB <sub>2</sub> -2	70.7 Cu-25.7 Zn-3.58 Al + 0.03 CrB <sub>2</sub>	136	620
XNiB-1	70.7 Cu-25.7 Zn-3.58 Al + 0.052 NiB	125	250
XNiB-2	70.7 Cu-25.7 Zn-3.58 Al + 0.034 NiB	124	300
XNiB-3	70.7 Cu-25.7 Zn-3.58 Al + 0.016 NiB	125	450
XZr-1	70.7 Cu-25.7 Zn-3.58 Al + 1.26 Zr	110	25
XZr-2	70.7 Cu-25.7 Zn-3.58 Al + 0.91 Zr	111	40
XZr-3	70.7 Cu-25.7 Zn-3.58 Al + 0.64 Zr	110	40
XZr-4	70.7 Cu-25.7 Zn-3.58 Al + 0.3 Zr	120	50
XTi-1	70.7 Cu-25.7 Zn-3.58 Al + 0.8 Ti	116	60
XTi-2	70.7 Cu-25.7 Zn-3.58 Al + 0.52 Ti	112	90
XTi-3	70.7 Cu-25.7 Zn-3.58 Al + 0.32 Ti	85	90
XTi-4	70.7 Cu-25.7 Zn-3.58 Al + 0.22 Ti	102	100
XCr-1	70.7 Cu-25.7 Zn-3.58 Al + 0.99 Cr	123	500
XCr-2	70.7 Cu-25.7 Zn-3.58 Al + 0.78 Cr	127	650
XCr-3	70.7 Cu-25.7 Zn-3.58 Al + 0.31 Cr	120	550
XV-1	70.7 Cu-25.7 Zn-3.58 Al + 1.25 V	106	300
XV-2	70.7 Cu-25.7 Zn-3.58 Al + 1.03 V	115	300
XV-3	70.7 Cu-25.7 Zn-3.58 Al + 0.72 V	109	500
XV-4	70.7 Cu-25.7 Zn-3.58 Al + 0.53 V	120	500
Y	65.6 Cu-31.4 Zn-2.95 Al + 0.1 Zr	< -192	130
YZr	65.6 Cu-31.4 Zn-2.95 Al + 1.1 Zr	-145	50
YTi	65.6 Cu-31.4 Zn-2.95 Al + 0.1 Zr - 1.1 Ti	-150	80
YCr	65.6 Cu-31.4 Zn-2.95 Al + 0.1 Zr - 1.1 Cr	-167	100
YV	65.6 Cu-31.4 Zn-2.95 Al + 0.1 Zr - 1.1 V	-165	350

<sup>a</sup> All alloys reported here were annealed at 800°C for 5 min.

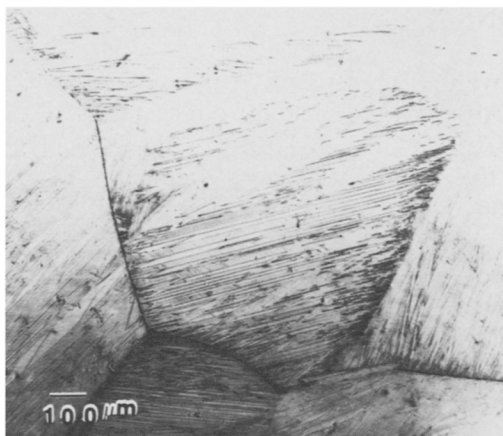


FIG. 1. Optical micrograph of 70.7% Cu-25.7% Zn-3.58% Al (alloy X) annealed at 800°C for 5 min. Average grain size ~900  $\mu\text{m}$ .

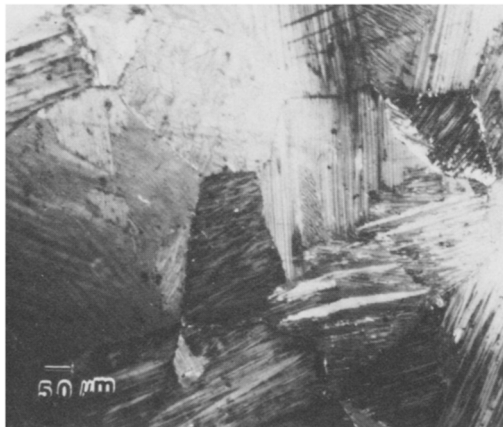


FIG. 2. Optical micrograph of alloy XB-1 (0.051% B) annealed at 800°C for 5 min. Average grain size ~250  $\mu\text{m}$ .

was noted in any of them. The addition of B thus resulted in some grain refinement, with the effect proportional to the amount of B added. The  $M_s$  temperature of XB-1 was shifted from 107°C to 120°C, and XB-3 had an  $M_s$  temperature of 133°C. The change of  $M_s$  temperature is thought to be due to a master alloy composition change during the remelting process, not a direct grain size refinement effect, even though the shift of transformation temperature was not dramatic.

## AlB<sub>2</sub> ADDITIONS

Three alloys with 0.051% AlB<sub>2</sub> (XAlB<sub>2</sub>-1), 0.03% AlB<sub>2</sub> (XAlB<sub>2</sub>-2), and 0.01% AlB<sub>2</sub> (XAlB<sub>2</sub>-3) were melted from a master alloy of composition of 70.7% Cu–25.7% Zn–3.58% Al–0.56% AlB<sub>2</sub>. After 5 min solution treatment at 800°C, the master alloy had a grain size of 70 μm. XAlB<sub>2</sub>-1 had a grain size of 300 μm, XAlB<sub>2</sub>-2, 640 μm; and XAlB<sub>2</sub>-3, 730 μm. Compared with the 1 mm grain size of the additive-free base alloy, some grain refinement resulted, although it was not very significant. All four AlB<sub>2</sub> alloys showed no observable second phase particles; therefore, the grain size refinement may be from dissolved AlB<sub>2</sub> in solid solution as reported for the Cu–Al–Ni system [1, 8]. For the master alloy containing 0.56% AlB<sub>2</sub>, the observed grain size of 70 μm represented a more than ten-fold reduction. The  $M_s$  temperatures for alloys XAlB<sub>2</sub>-1, XAlB<sub>2</sub>-2, and XAlB<sub>2</sub>-3 were all about 130°C. As grain refinement in these three alloys was small, the small shift of transformation temperature may be due to a compositional change during the remelting process. Figure 3 shows the 0.03% AlB<sub>2</sub>-doped alloy after annealing at 800°C for 5 min.

## TiB<sub>2</sub> ADDITIONS

Three alloys with 0.051% TiB<sub>2</sub> (XTiB<sub>2</sub>-1), 0.03% TiB<sub>2</sub> (XTiB<sub>2</sub>-2), and 0.01% TiB<sub>2</sub> (XTiB<sub>2</sub>-3) were melted from a master alloy of composition 70.7% Cu–25.7% Zn–3.58% Al–0.6% TiB<sub>2</sub>. After 5 min of solution treatment at 800°C, the master alloy had a grain size of 580 μm; XTiB<sub>2</sub>-1, 760 μm; XTiB<sub>2</sub>-2, 780 μm; and XTiB<sub>2</sub>-3, 900 μm. These were not much different from the base alloy, which had a grain size of 1 mm. A small fraction of second-phase particles was observed both at the grain boundaries and in the matrix, as seen in Fig. 4. Similar second-phase particles (X phase) were reported in Ti-doped Cu–Al–Ni alloys [1, 7, 8] and in Ti-doped Cu–Zn–Al alloys in the present study. Other work [1, 7] on Ti-doped Cu–Al–Ni alloys reported that the particles were a Ti-rich second phase that was not restricted to the grain boundaries and thus was not believed to be a major factor in grain size refinement. The  $M_s$  temperatures of XTiB<sub>2</sub>-1, XTiB<sub>2</sub>-2, XTiB<sub>2</sub>-3, and the master alloy were all in the range 130–140°C. This is believed due to some compositional change in the master alloy during the remelting process.

## CrB<sub>2</sub> ADDITIONS

Two alloys containing 0.052% CrB<sub>2</sub> (XCrB<sub>2</sub>-1) and 0.03% CrB<sub>2</sub> (XCrB<sub>2</sub>-2) were melted from a master alloy of composition 70.7% Cu–25.7% Zn–

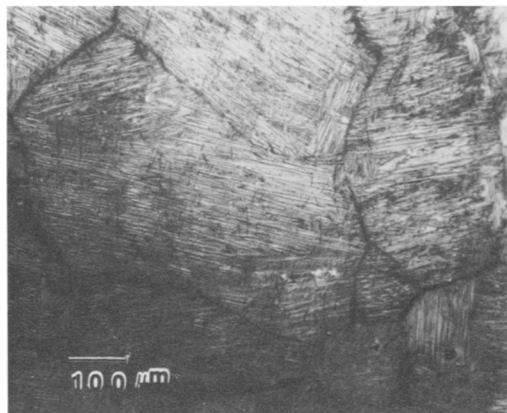


FIG. 3. Optical micrograph for alloy XAlB<sub>2</sub>-2 (0.03% AlB<sub>2</sub>) annealed at 800°C for 5 min. Average grain size ~640 μm.

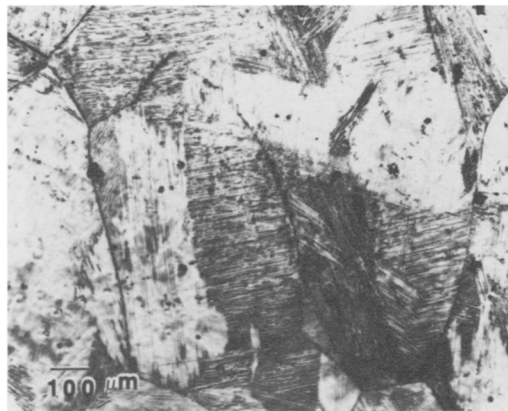


FIG. 4. Optical micrograph for alloy XTiB<sub>2</sub>-1 (0.051% TiB<sub>2</sub>) annealed at 800°C for 5 min. Average grain size ~760 μm.

3.58% Al–0.64% CrB<sub>2</sub>. After 5 min solution treatment at 800°C, the master alloy had a grain size of 130 μm, XC<sub>r</sub>B<sub>2</sub>-1 had a grain size of 550 μm, and XC<sub>r</sub>B<sub>2</sub>-2 had a grain size of 620 μm. The master alloy showed more grain refinement than the dilute alloys. All three alloys had an  $M_s$  temperature of 135°C. A small fraction of second phase was observed both at grain boundaries and in the matrix, as seen in Fig. 5.

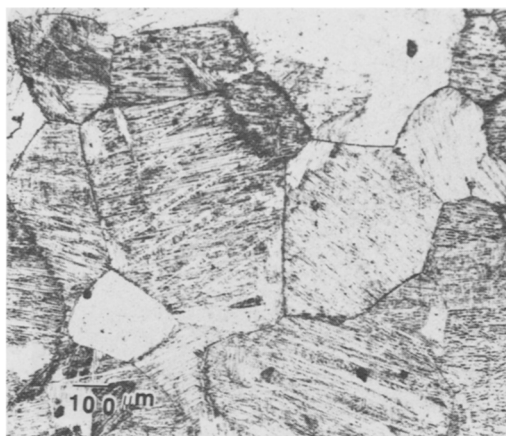


FIG. 5. Optical micrograph for alloy XCrB<sub>2</sub>-2 (0.03% CrB<sub>2</sub>) annealed at 800°C for 5 min. Average grain size ~600 μm.

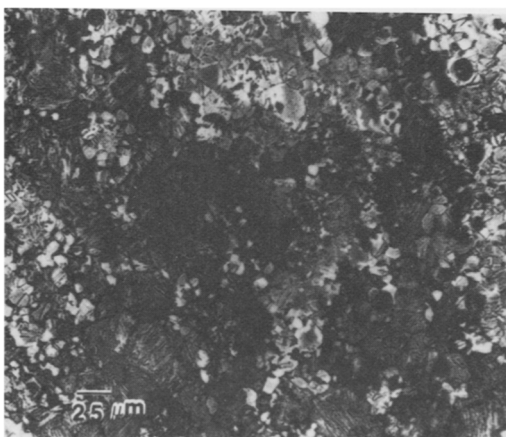


FIG. 6. Optical micrograph for master alloy of NiB (0.64% NiB) annealed at 800°C for 5 min. Average grain size 25 μm.

## NiB ADDITIONS

Three alloys containing 0.052% NiB (XNiB-1), 0.034% NiB (XNiB-2), and 0.016% NiB (XNiB-3) were melted from a master alloy of composition 70.7% Cu-25.7% Zn-3.58% Al-0.64% NiB. After 5 min solution treatment at 800°C, the master alloy had a grain size 25 μm (Fig. 6), showing remarkable refinement compared with the 1 mm grain size of the base

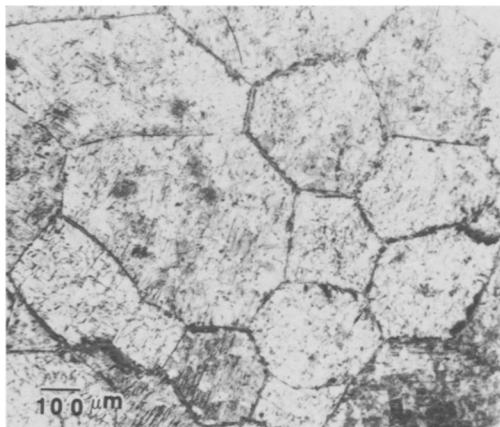


FIG. 7. Optical micrograph of alloy XNiB-2 (0.034% NiB) annealed at 800°C for 5 min. Average grain size ~300  $\mu\text{m}$ .

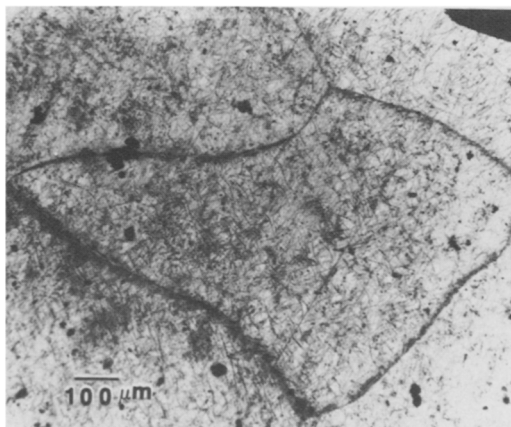


FIG. 8. Optical micrograph of alloy XNiB-2 (0.034% NiB) annealed at 800°C for 1 h. Average grain size ~1 mm.

alloy under the same annealing condition. Alloy XNiB-1 had a grain size of about 250  $\mu\text{m}$ , XNiB-2, 300  $\mu\text{m}$ ; and XNiB-3, 450  $\mu\text{m}$ . However, the grain growth rate of these alloys was very fast. Upon increasing the solution-treatment time at 800°C from 5 min to 0.5 h, alloy XNiB-1 achieved a grain size about 800  $\mu\text{m}$ , with an  $M_s$  temperature at 125°C. After 1 h solution treatment at 800°C, all three NiB-doped alloys had grain sizes larger than 1 mm (Figs. 7 and 8). But the alloys with larger grain sizes still had  $M_s$  temperatures between 125°C and 128°C.

## Zr ADDITIONS

Zr was added to the two base alloys, X and Y, of which alloy Y already contained 0.1% Zr.

Four different Zr concentrations, 1.26% (XZr-1), 0.91% (XZr-2), 0.64% (XZr-3), and 0.3% (XZr-4) were added to alloy X (original composition 70.7% Cu–25.7% Zr–3.58% Al). After 5 min solution treatment at 800°C, XZr-1 had a grain size of 25 µm and XZr-2, XZr-3, and XZr-4, had grain sizes of 40 µm, 40 µm, and 50 µm, respectively. The grain size reduction was proportional to the amount of Zr added, unlike the case for additions of Zr to a Cu–Al–Ni alloy [8]. In the Cu–Al–Ni alloy, the degree of grain size refinement was independent of the amount of Zr-doping once a certain level was reached [8]. Upon increasing the solution-treatment time to 0.5 h, the grain growth rates for the four Zr-doped alloys were very slow. XZr-1 had a grain size of 30 µm, and XZr-2, XZr-3, XZr-4 had grain sizes of 40 µm, 60 µm, and 70 µm, respectively. Compared with the 1 mm grain size of the base alloy under similar annealing conditions, this is a very significant reduction. Furthermore, after 3 h solution treatment at 800°C, XZr-1 had a grain size of 40 µm, and XZr-2, XZr-3 and XZr-4 had grain sizes of 40 µm, 80 µm, and 90 µm, respectively. With the same solution treatment, the base alloy would have a grain size in the range of 3 mm, as shown in Fig. 9. Therefore, Zr-doping of Cu–Zn–Al SMA not only refined the grain size, but also suppressed the grain growth rate to virtually zero. Second-phase particles were observed in all four Zr-doped alloys, as seen in Fig. 10. Zr- and Ti-rich second-phase particles have also been reported for Cu–Al–Ni alloys [1, 7, 8], both at grain boundaries and within the grains. In the present case, most second-phase particles were concentrated at grain boundaries, as shown in Fig. 10. These second-phase particles were evidently responsible for the suppression of grain growth in the Zr-doped Cu–Zn–Al alloys.

The  $M_s$  temperatures of the four Zr-doped alloys were in the range 110–120°C, compared with the range of 107°C (5 min solution treatment at 800°C) to 111°C (3 h solution treatment) of the base alloy. The shape memory effect was not modified by doping. A one-step melting process was used to make all four Zr-doped Cu–Zn–Al alloys. Thus, any changes in chemical composition were expected to be minimal. This provides further evidence that the  $M_s$  temperature shift found for other dopants added to Cu–Zn–Al alloys resulted essentially from chemical compositional changes in the master alloy during remelting.

Alloy YZr, with 1.1% Zr, showed a grain size of 50 µm after 6 h solution treatment at 800°C, compared with a 280 µm grain size for the base alloy Y (which already contained 0.1% Zr) under identical annealing conditions

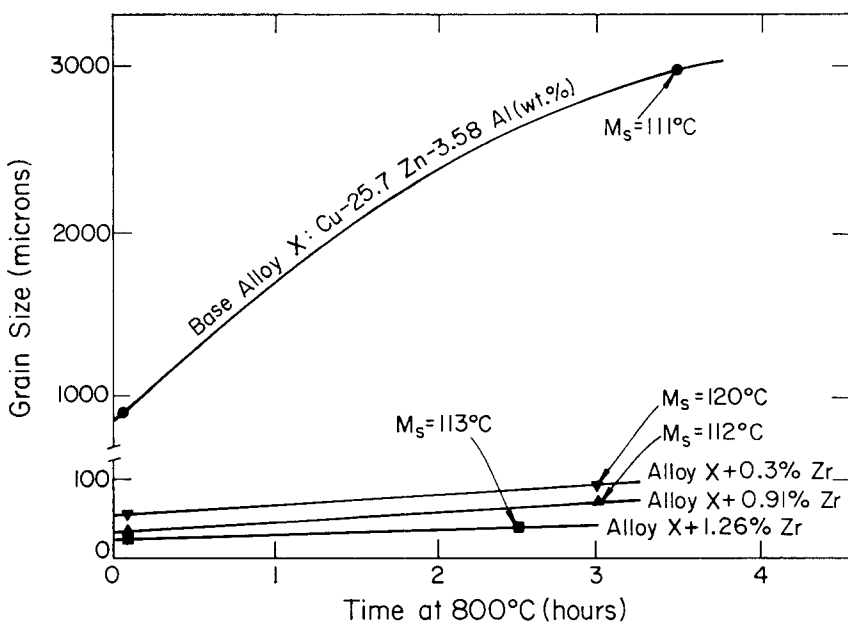


FIG. 9. Grain growth rate for dopant-free alloy X and Zr-doped alloy X.

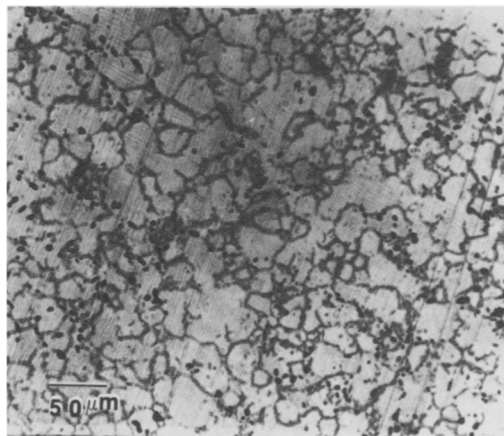


FIG. 10. Optical micrograph of alloy XZr-2 (0.91% Zr) annealed at 800°C for 2.5 h. Average grain size  $\sim 40 \mu\text{m}$ .

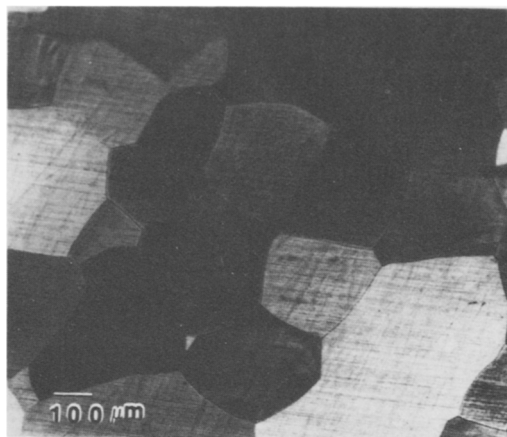


FIG. 11. Optical micrograph of alloy Y, annealed at 800°C for 6 h. Average grain size ~280 μm.

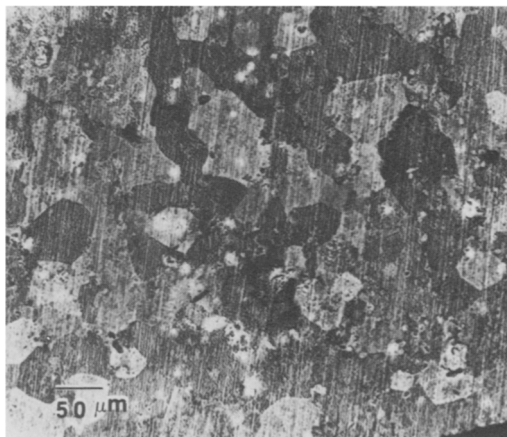


FIG. 12. Optical micrograph of alloy YZr (1.1% Zr) annealed at 800°C for 6 h. Average grain size ~50 μm.

(Figs. 11 and 12). More concentrated Zr alloys would further reduce the grain size and suppress the grain growth rate. The  $M_s$  temperature of YZr was increased to -144°C from the -192°C recorded with alloy Y.

#### Ti ADDITIONS

Four different concentrations of Ti, 0.8% (XTi-1), 0.52% (XTi-2), 0.32% (XTi-3), and 0.22% (XTi-4), were added to alloy X. Grain sizes were

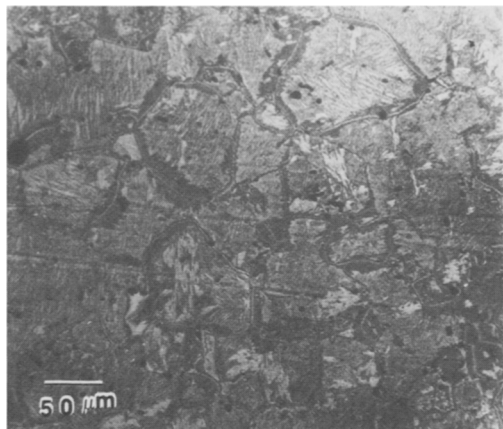


FIG. 13. Optical micrograph of alloy XTi-1 (0.8% Ti) annealed at 800°C for 1 h. Average grain size  $\sim 80 \mu\text{m}$ . A grain boundary anomaly is observed.

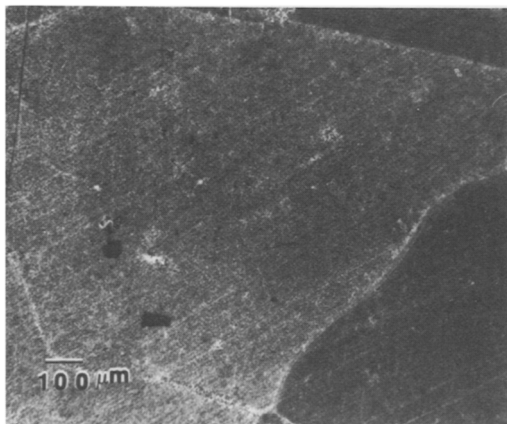


FIG. 14. Optical micrograph for alloy XTi-1 (0.8% Ti) annealed at 800°C for 16 h. Average grain size  $> 1 \text{ mm}$ . The grain boundary anomaly has disappeared.

reduced to less than 100  $\mu\text{m}$  for all four alloys after 5 min solution treatment (Fig. 13). However, after 3 h solution treatment, the grains grew to the range of 200  $\mu\text{m}$  to 300  $\mu\text{m}$  for alloys XTi-1 and XTi-2. For the more dilute alloys, XTi-3 and XTi-4, the grains grew to the range of 800  $\mu\text{m}$ . The grain refinement effect of Ti was thus good for only shorter solution treatment times. However, the grain growth rate was somewhat larger for these alloys, especially the more dilute ones. The grain boundary anomaly observed after short-period annealing (Fig. 13) disappeared upon increasing the annealing time (Fig. 14). It is therefore concluded that the

grain boundary anomaly was responsible for the initial grain size reduction, but had no effect in suppressing subsequent grain growth.  $M_s$  temperatures were kept in the range between 100°C and 165°C, except for alloy XTi-3, which had an  $M_s$  temperature of 85°C.

Alloy YTi with 1.1% Ti was melted using base alloy Y. YTi had a grain size of 80  $\mu\text{m}$  after 6 h annealing at 800°C, compared with 280  $\mu\text{m}$  for the base alloy for the same annealing condition. The  $M_s$  temperature was increased to -150°C.

## V ADDITIONS

Four alloys containing 1.25% V (XV-1), 1.03% V (XV-2), 0.72% V (XV-3), and 0.53% V (XV-4) were melted using alloy X. The initial grain refinement effect of V was not as good as for other pure dopants, such as Zr and Ti. For the more concentrated alloys XV-1 and XV-2, a grain size of 300  $\mu\text{m}$  was obtained after 0.5 h solution treatment at 800°C, but larger grain sizes of 600  $\mu\text{m}$  were obtained after 1 h or 2 h solution treatment (Figs. 15 and 16). For the more dilute alloys, XV-3 and XV-4, no grain refinement was observed at all. The degree of grain size reduction at shorter annealing periods was identical to the results reported by Enami et al. [5], who reported an average grain size of 300  $\mu\text{m}$  after about 0.5 h annealing. The  $M_s$  temperature of all four V-doped alloys varied little.

Alloy YV with 1.1% V was melted from base alloy Y. Contrary to previous results, the grain size of alloy YV was larger than that for base alloy Y. A grain size of 350  $\mu\text{m}$  was observed after 5 min of solution treatment at 800°C. The  $M_s$  temperature was increased to -165°C.

## Cr ADDITIONS

Three alloys with 0.99% Cr (XCr-1), 0.78% Cr (XCr-2), and 0.31% Cr (XCr-3) were prepared from base alloy X. Grain refinement was not significant. Grain sizes in the range of 500  $\mu\text{m}$  were obtained for all three alloys when annealed only 5 min at 800°C. Moreover, the grain growth rates of all alloys were very fast. After only 0.5 h annealing at 800°C, a 1 mm grain size was observed in all three alloys.

Alloy YCr with 1.1% Cr was melted using alloy Y. A grain size of 150  $\mu\text{m}$  was obtained after 6 h solution treatment at 800°C. Compared with base alloy Y, adding Cr did not further reduce the grain size, although it did somewhat suppress the grain growth rate. The  $M_s$  temperature was increased to -167°C.

All the alloys discussed above were rolled in air to form plate of thick-

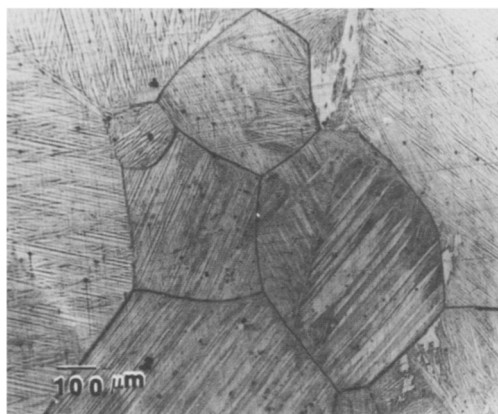


FIG. 15. Optical micrograph of alloy XV-1 (1.25% V) annealed at 800°C for 0.5 h. Average grain size ~300  $\mu\text{m}$ .

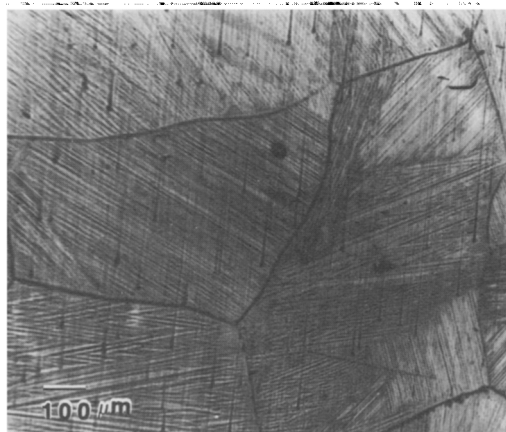


FIG. 16. Optical micrograph of alloy XV-1 (1.25% V) annealed at 800°C for 1 h. Average grain size ~600  $\mu\text{m}$ .

ness of 1.27 mm. Intermediate annealing at 600°C was required every two to three passes. Each pass used a reduction rate of about 3–5%. The final reduction for each alloy was about 83%. However, it was possible to obtain 98% reduction for a final thickness of 0.254 mm for all alloys. Figure 17 shows that the 0.91% Zr-doped alloy (XZr-2) had a grain size of 70  $\mu\text{m}$  after rolling to a thickness of 0.254 mm and then annealing at 800°C for 0.5 hr. Rolling did not enhance the grain growth for Zr-doped Cu-Zn-Al

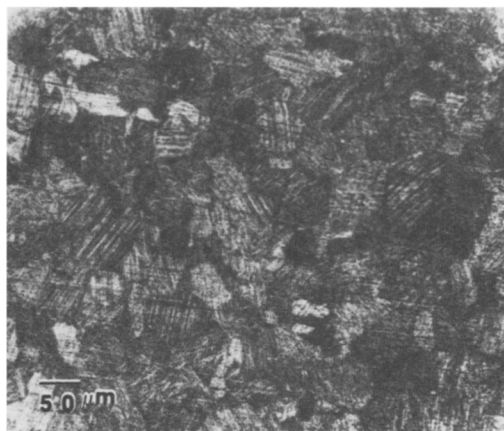


FIG. 17. Optical micrograph of alloy XZr-2 (0.91% Zr) rolled to 0.254 mm thickness and annealed at 800°C for 0.5 h. Average grain size ~70 μm.

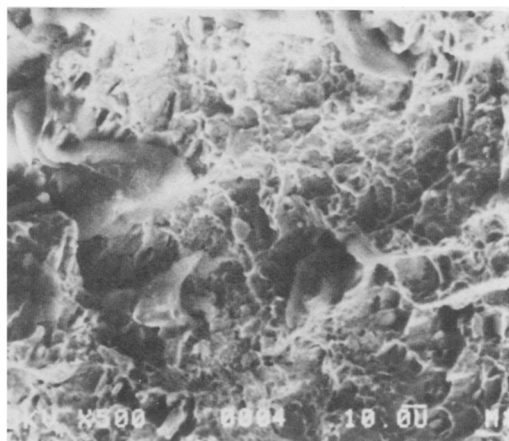


FIG. 18. SEM micrograph of alloy XZr-2 (0.91% Zr) annealed at 800°C for 1.5 h and impact fractured in situ in Auger vacuum system at room temperature.

alloys. Alloys containing Cr were more brittle, and cracks were easily induced using similar rolling schedules.

Zr-, Ti-, V-, and Cr-doped alloys were fractured using an Instron machine at room temperature in air (below the  $M_s$  temperature) and the fracture surfaces were subsequently examined by SEM. Two alloys containing Zr and Ti were also fractured in an Auger electron vacuum system and immediately examined by Auger analysis in order to study any pos-

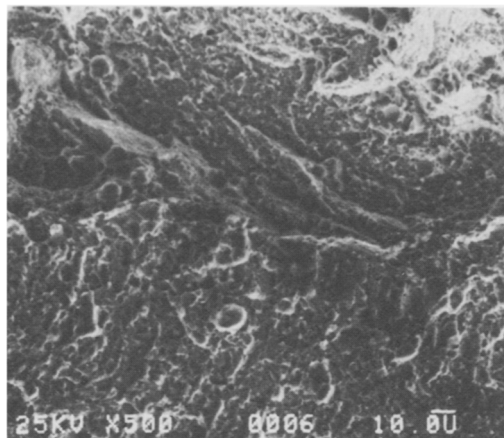


FIG. 19. SEM micrograph of alloy XTi-2 (0.52% Ti) annealed at 800°C for 1.5 h and impact fractured in situ in Auger vacuum system at room temperature.

sible grain boundary segregation. The alloys examined showed a transgranular fracture mode with river patterns, with some areas showing dimples (Figs. 18 and 19). The dimples are believed due to the presence of second-phase particles in both the Zr- and the Ti-doped Cu-Zn-Al alloys. A refined grain size can change the grain boundary orientation over short distances and therefore the crack propagation path along grain boundaries can be easily disrupted. In polycrystalline specimens of the Cu-based  $\beta$ -brass-type SMA, the intrinsic large grain size and high elastic anisotropy lead usually to an intergranular fracture mode and poor mechanical properties. From present results, additions of dopants to Cu-Zn-Al alloys enhance the ductile transgranular fracture mode. Similar results were also reported in V-doped Cu-Zn-Al [5] alloys and Ti- or Zr-doped Cu-Al-Ni alloys [1, 8]. Auger electron analysis of the Ti- and Zr-doped Cu-Zn-Al alloys did not reveal significant grain boundary segregation.

Preliminary TEM work was performed on Ti-doped alloys. Very fine, unidentified, precipitates were observed in the martensitic phase.

Alloy compositions are very important with respect to the martensitic transformation temperature in Cu-based SMA. An effort was made to relate the  $M_s$  temperature to alloy composition in the Cu-Zn-Al system. From various reports in the literature, 138  $M_s$  temperatures for different Cu-Zn-Al compositions were collected. A computer program involving a first-order linear regression model using two independent variables (concentrations of Zn and Al) was used to establish a relationship. The best relationship between Zn and Al contents and the  $M_s$  temperatures in the

Cu-Zn-Al system was found to be:

$$M_s \text{ (°C)} = 1890 - 51.0\text{Zn (wt.\%)} - 134.5\text{Al (wt.\%)}$$

Using this relationship, which predicts the  $M_s$  temperature to  $\pm 5^\circ\text{C}$ , it is possible to estimate the shape memory effect in the Cu-Zn-Al system reasonably accurately before the alloys are melted.

## **Summary**

The effect of additions of a fourth element on the grain refinement in two commercial ternary Cu-Zn-Al alloys has been studied by optical microscopy, electrical resistivity measurements, and Auger electron analysis. The results obtained can be summarized as follows.

1. Grain refinement with boron and various boride additions was not very significant. Grain growth rates for the boron-doped alloys were relatively large.
2. Additions of pure metallic elements were quite effective in grain refinement. Zr- and Ti-doped alloys had grain sizes as small as 25–30  $\mu\text{m}$ , which represents a reduction of some 40 times. Zr suppressed the subsequent grain growth rate to virtually zero.
3. Second-phase particles were observed at the grain boundaries in Zr-doped alloys. These are believed to be responsible for the suppression in grain growth.
4. The  $M_s$  temperatures of all alloys studied were not dramatically changed by quaternary additions. Some slight modification of the  $M_s$  temperatures in certain alloys were observed and are believed due to small compositional changes in the master alloys during remelting, rather than from grain refinement by the various dopants.
5. Good formability was obtained for all alloys studied. All showed a ductile transgranular fracture mode.

*Financial support from the IBM-SURS Program is gratefully acknowledged. Auger electron and scanning electron microscope analyses were conducted in the Center for Microanalysis of Materials, University of Illinois at Urbana-Champaign, supported by the DOE under contract De-AC02-76ER01198. Special thanks are due to Ms. Nancy Finnegan for her assistance in performing the Auger electron analysis.*

## **References**

1. G. N. Sure and L. C. Brown, The mechanical properties of grain refined  $\beta$ -CuAlNi strain memory alloys, *Met. Trans.* 15A:1613 (1984).

2. S. Miyazaki, K. Otsuka, H. Sakamoto, and K. Shimizu, The Fracture of a Cu-Al-Ni shape memory alloy, *Trans. Japan Inst. Metals* 4:244 (1981).
3. T. J. Gann, *The Effects of Grain Size on the Martensite Transformation in Cu-Zn-Al Shape Memory Alloys*, M.S. Thesis, Naval Postgraduate School, Monterey, CA. Dec. 1982.
4. Y. Hanatate, M. Miyagi, T. Hamada, and F. Uratani, *The Effects of Boron on Grain Refinement in Cu-Al-Ni Alloys*, Report of Osaka Industrial Technical Research Institute No. 81, (1982) 17, in Japanese.
5. K. Enami, N. Takimoto, and S. Nenno, Effect of vanadium addition on the grain size and mechanical properties of the Cu-Al-Zn shape memory alloys, in *Proc. ICOMAT-82* (L. Delaey and M. Chandrasekaran, Eds.), Leuven, Belgium (1982), pp. c4-773.
6. D. N. Adnyana, Presentation at informal meeting on shape memory alloys in Leuven, Belgium, June, 1984.
7. S. Sugimoto, K. Kamei, H. Matsumoto, S. Komatsu, A. Akamatsu, and T. Sugimoto, Grain refinement and the related phenomena in quaternary Cu-Al-Ni-Ti shape memory alloys, in *Proc. ICOMAT-82* (L. Delaey and M. Chandrasekran, Eds.), Leuven, Belgium (1982), pp. c4-761.
8. J. S. Lee and C. M. Wayman, Grain refinement of a Cu-Al-Ni shape memory alloy by Ti and Zr additions, (to be published).

Received February 1986; accepted March 1986.